ORIGINAL ARTICLE

A Chronic Obstructive Pulmonary Disease Susceptibility Gene, *FAM13A*, Regulates Protein Stability of β-Catenin

Zhiqiang Jiang[1], Taotao Lao[1], Weiliang Qiu[1], Francesca Polverino[2,3], Kushagra Gupta[2], Feng Guo[1], John D. Mancini[1], Zun Zar Chi Naing[1], Michael H. Cho[1,2], Peter J. Castaldi[1,4], Yang Sun[2], Jane Yu[2], Maria E. Laucho-Contreras[2], Lester Kobzik[5], Benjamin A. Raby[1,2], Augustine M. K. Choi[6], Mark A. Perrella[2,7], Caroline A. Owen[2,3], Edwin K. Silverman[1,2], and Xiaobo Zhou[1,2]

[1]Channing Division of Network Medicine, Department of Medicine, [2]Division of Pulmonary and Critical Care Medicine, Department of Medicine; [4]Division of General Internal Medicine, Department of Medicine, and [7]Pediatric Newborn Medicine, Brigham and Women's Hospital and Harvard Medical School, Boston, Massachusetts; [3]The Lovelace Respiratory Research Institute, Albuquerque, New Mexico; [5]Department of Pathology, Brigham and Women's Hospital, Boston, Massachusetts; and [6]Department of Medicine, Weill Cornell Medical College, New York, New York

Abstract

Rationale: A genetic locus within the *FAM13A* gene has been consistently associated with chronic obstructive pulmonary disease (COPD) in genome-wide association studies. However, the mechanisms by which *FAM13A* contributes to COPD susceptibility are unknown.

Objectives: To determine the biologic function of *FAM13A* in human COPD and murine COPD models and discover the molecular mechanism by which *FAM13A* influences COPD susceptibility.

Methods: *Fam13a* null mice (*Fam13a*$^{-/-}$) were generated and exposed to cigarette smoke. The lung inflammatory response and airspace size were assessed in *Fam13a*$^{-/-}$ and *Fam13a*$^{+/+}$ littermate control mice. Cellular localization of FAM13A protein and mRNA levels of *FAM13A* in COPD lungs were assessed using immunofluorescence, Western blotting, and reverse transcriptase–polymerase chain reaction, respectively. Immunoprecipitation followed by mass spectrometry identified cellular proteins that interact with FAM13A to reveal insights on FAM13A's function.

Measurements and Main Results: In murine and human lungs, *FAM13A* is expressed in airway and alveolar type II epithelial cells and macrophages. *Fam13a* null mice (*Fam13a*$^{-/-}$) were resistant to chronic cigarette smoke–induced emphysema compared with *Fam13a*$^{+/+}$ mice. *In vitro*, FAM13A interacts with protein phosphatase 2A and recruits protein phosphatase 2A with glycogen synthase kinase 3β and β-catenin, inducing β-catenin degradation. *Fam13a*$^{-/-}$ mice were also resistant to elastase-induced emphysema, and this resistance was reversed by coadministration of a β-catenin inhibitor, suggesting that FAM13A could increase the susceptibility of mice to emphysema development by inhibiting β-catenin signaling. Moreover, human COPD lungs had decreased protein levels of β-catenin and increased protein levels of FAM13A.

Conclusions: We show that FAM13A may influence COPD susceptibility by promoting β-catenin degradation.

Keywords: *FAM13A*; β-catenin; protein stability; emphysema; cell proliferation

(Received in original form May 24, 2015; accepted in final form January 21, 2016)

Supported by National Institutes of Health grants R01 HL075478, P01 HL105339, and R01HL111759 (E.K.S.), R01HL127200 and R21HL120794 (X.Z.), R01 AI111475-01 and R21 HL111835 (C.A.O.), and YFEL141004 (F.P.); the Flight Attendants Medical Research Institute CIA#123046 (C.A.O.); and Brigham and Women's Hospital and Lovelace Respiratory Research Institute Research Consortium (C.A.O).

Author Contributions: Study design: X.Z. and Z.J. Statistical analysis: W.Q., X.Z., and E.K.S. Affinity purification–mass spectrometry and data analysis: Z.J. and X.Z. Western blot and pull-down assays: Z.J. Real-time polymerase chain reaction: Z.J. Immunofluorescence staining in human tissue: F.P. and C.A.O. Immunofluorescence staining in murine lung samples: Z.J. Immunohistochemistry staining: Z.J., F.G., Y.S., and J.Y. Cigarette smoke murine model and data analysis: K.G., M.E.L.-C., Z.J., J.D.M., and Z.Z.C.N. Elastase murine model and data analysis: Z.J. and T.L. Genetics study support: M.H.C., P.J.C., E.K.S., and X.Z. Pathology: L.K. Manuscript writing: X.Z., Z.J., L.K., A.M.K.C., B.A.R., M.A.P., C.A.O., and E.K.S.

Correspondence and requests for reprints should be addressed to Xiaobo Zhou, Ph.D., Brigham and Women's Hospital, Harvard Medical School, Channing Division of Network Medicine, Boston, MA 02115. E-mail: xiaobo.zhou@channing.harvard.edu.

This article has an online supplement, which is accessible from this issue's table of contents at www.atsjournals.org

Am J Respir Crit Care Med Vol 194, Iss 2, pp 185–197, Jul 15, 2016

Originally Published in Press as DOI: 10.1164/rccm.201505-0999OC on February 10, 2016
Internet address: www.atsjournals.org

At a Glance of Commentary

Scientific Knowledge on the Subject: Genome-wide association studies (GWASs) have been successful in identifying genomic regions associated with chronic obstructive pulmonary disease. However, the identification of the key genes within those GWAS regions and their biologic impact requires further investigation.

What This Study Adds to the Field: Our research provides a functional study on *FAM13A*, a chronic obstructive pulmonary disease GWAS region gene, and reveals that the molecular mechanism by which FAM13A influences chronic obstructive pulmonary disease susceptibility is likely through interacting with PP2A/β-catenin, thus promoting degradation of β-catenin.

Chronic obstructive pulmonary disease (COPD), the third leading cause of death in the United States (1, 2), is characterized by emphysematous destruction of the alveoli and thickening of the airway walls in response to chronic cigarette smoke (CS) exposure. Although the dose-response relationship between cigarette smoking and pulmonary function levels is well-established, there is considerable variability in the reduction in pulmonary function among smokers with similar smoking exposures (3, 4). The low percentage of variance in pulmonary function explained by smoking suggests that there could be differences in genetic susceptibility to the effects of cigarette smoking (5, 6). Genome-wide association studies (GWASs) provide an unbiased and comprehensive approach to search for common genetic susceptibility loci throughout the genome in thousands of subjects (7, 8). These studies have successfully identified susceptibility loci for many complex diseases (9, 10). The *FAM13A* gene (family with sequence similarity 13, member A) has been consistently associated with COPD by GWAS (11, 12), but the molecular mechanisms and biologic functions of *FAM13A* remain largely unexplored.

The central molecule in the Wnt pathway, β-catenin, is normally maintained at low levels in the cytosol because of its association with a destruction complex, including glycogen synthase kinase 3β (GSK-3β), which phosphorylates β-catenin for rapid degradation via ubiquitin-dependent proteolysis (13, 14). Upon stimulation by Wnt ligands, β-catenin is stabilized and then translocates to the nucleus, where it binds to T-cell factor/lymphoid enhancer factor (TCF/LEF) transcription factors, activating the expression of Wnt target genes, promoting cell proliferation (15–17) and limiting cell differentiation (16, 18), thus contributing to both airway (18, 19) and alveolar epithelial repair (20–22) after injury. Consistent with this concept, activation of β-catenin signaling by lithium chloride attenuated elastase-induced experimental emphysema (21), suggesting that β-catenin signaling contributes to lung repair/regeneration in response to various injuries.

Herein, we used complementary *in vivo* and *in vitro* approaches coupled with studies of human COPD samples to provide evidence that FAM13A influences COPD susceptibility by promoting β-catenin degradation. Some of the results of this study have been previously reported in the form of an abstract (23).

Methods

Human Tissues

Studies of human samples were approved by the Partners Human Research Committee (Boston, MA). Sections of lung were obtained from lung biopsies or from explanted lungs from patients with COPD provided by the NHLBI-sponsored Lung Tissue Research Consortium (LTRC) or Pulmonary and Critical Care Medicine Human Biorepository at Brigham and Women's Hospital. Deidentified specimens were used in all of our assays. The localization of FAM13A in human lungs was examined using immunofluorescence staining of formalin-fixed and paraffin-embedded lung sections. Expression levels of β-catenin and FAM13A were assessed in human lung sections as described previously (24). Subjects with very severe COPD had FEV_1 less than 40% predicted (*see* Table E2 in the online supplement). All of the demographic and clinical data were provided by the LTRC.

Generation of *Fam13a*$^{-/-}$ Mice

All animal studies were approved by the Institutional Animal Care and Use Committee, Harvard Medical School. Murine embryonic stem cells (JM8.N4 bought from the knockout mouse project repository, now the International Mouse Phenotype Consortium, project #70561) transfected with a *Fam13a* gene-targeted mutant construct (25) were injected into C57BL/6 host embryos to generate *Fam13a* mutant chimeric mice that were then bred with C57BL/6 wild-type mice to obtain germ-line transmission of the mouse *Fam13a* mutant allele. All mice were housed in the animal facility of Harvard Medical School with a 12-hour light/12-hour dark cycle. Five *Fam13a*$^{-/-}$ mice at 2 months of age were harvested and major organs were removed. Organ sections were assessed by a senior pathologist (L.K.) to determine whether there were any abnormalities in major organs (lung, kidney, intestine, liver, and heart) (*see* Figure E2).

CS Exposure of Mice

Female *Fam13a*$^{-/-}$ and *Fam13*$^{+/+}$ (∼10 wk old) mice were exposed to mixed main-stream and side-stream CS from 3R4F Kentucky Research cigarettes for 5 days/week in Teague TE 10z (Teague Enterprises, Woodland, CA) chambers (tobacco smoke pollution ∼100–200 mg/m^3 and CO levels ∼6 parts per million). As a control, mice were exposed to filtered air (air) for the same time period. At the end of the exposure period, mice were killed by CO_2 narcosis and cervical dislocation before lung removal. Mice exposed to CS or air for 1 month and 6 months were harvested in a blinded way for subsequent analysis. We excluded two mice in the *Fam13a*$^{+/+}$ air group and one mouse in *Fam13a*$^{-/-}$ CS group because of poor inflation for mean chord length analysis. Quality of lung inflation was judged by a senior investigator blinded to the experimental condition (26, 27).

Cell Lines and Plasmids

All cell lines were purchased from American Type Culture Collection (ATCC, Manassas, VA). Human bronchial epithelial cells (16HBE cells) and embryonic kidney epithelial cells (HEK 293) were cultured in Eagle's minimal essential medium or Dulbecco's modified Eagle medium, respectively, supplemented with 10% fetal bovine serum, penicillin (50 units/ml), and streptomycin (50 μg/ml). For isolation of murine airway epithelial cells, mice were killed followed by immediate trachea removal. The trachea was then incubated in

15% pronase solution (Roche GmbH, Indianapolis, IN) overnight at 4°C. The next day, the digestion buffer was neutralized by 10% fetal bovine serum before three times of washing with Ham's F12 media. Cell suspensions were centrifuged and then incubated with DNase-I (0.5 g/L) for 5 minutes on ice. Cells were then seeded on a 10-cm cell culture plate coated with rat-tail type I collagen (50 μg/cm^2; BD Sciences, Franklin Lakes, NJ) and cultured in bronchial epithelial cell medium (ATCC) supplemented with bronchial epithelial cell growth kit (ATCC). Cells younger than passage 2 were used for experiments. Testing for *Mycoplasma* infection was performed routinely using Mycoalert Detection Kit from Lonza (LT07–218; Lonza, Hopkinton, MA) in cells used in this study.

Full-length human FAM13A (NP_001252507.1) and β-catenin (NP_001091679.1) were cloned into pCMV6-Entry Vector (Origene, Rockville, MD) with C-terminus FLAG and c-MYC tags and pmCherry.C1 vector with N-terminal mCherry tag. TOPFLASH and TK-rennila reporter plasmids were gifts from Dr. Ningzhi Xu (Chinese Academy of Medical Sciences and Peking Union Medical College) (28). The constitutively active mutant β-catenin (β-catenin::CS2) construct was a gift from Dr. Xingbin Ai (Harvard Medical School) (http://sitemaker.umich.edu/dlturner.vectors/home).

Statistical Methods

Statistical analysis for all pair-wise comparisons other than cell growth curve and β-catenin half-life measurement was performed using unpaired Student's *t* test with equal variances for all measurements. If normality assumption is violated, then Wilcoxon rank sum test was used.

For cell growth curve, we performed linear regression for each growth curve with cell count as outcome and day as predictor. We then tested if the slope of one growth curve is equal to that of another growth curve using a *Z* test constructed based on the estimated slopes and their standard errors. In addition, we checked the log-transformed growth curves and found growth curves on the original scale were closer to linear than log transformed growth curves. Hence, we used the original scale in our analyses. Reductions in β-catenin levels in nontargeting control short hairpin RNA (NT-shRNA) and FAM13A shRNA cells in Figure 2G were compared based on linear mixed effects model. Detailed METHODS are available in the online supplement.

Results

FAM13A Determines Susceptibility to Emphysema in Murine Models

FAM13A has been repeatedly identified in COPD GWA studies. However, the molecular mechanism by which FAM13A determines COPD susceptibility remains unclear. First, we stained FAM13A in human COPD lung sections to determine the tissue localization of FAM13A. Human airway cells positive for mucin 5AC (MUC5AC, mucosal cells), Club cell 10 KD protein (Club cells), or pan-cytokeratin (airway epithelial cells) and alveolar cells positive for surfactant protein-C (alveolar type II cells) express FAM13A in healthy smokers and COPD subjects (Figure 1A; *see* Figure E1A). Furthermore, FAM13A staining was also detected in CD14-positive alveolar macrophages (*see* Figure E1A). Immunofluorescence staining in murine lungs demonstrated the localization of Fam13a in airway epithelial cells staining positively for Club cell 10 KD protein and alveolar type II epithelial cells staining positively for surfactant protein-C (*see* Figure E1B). Both of these cell types are important for lung repair/regeneration (29, 30).

To determine the *in vivo* function of FAM13A, we generated *Fam13a* null mice (*Fam13a*$^{-/-}$) by targeting exon 5 of the murine *Fam13a* gene on a C57BL/6J background. We detected no expression of *Fam13a* in murine lungs from *Fam13a*$^{-/-}$ mice at both mRNA and protein levels (*see* Figures E2A and E2B). *Fam13a*$^{-/-}$ mice are viable and showed no gross defects in major organs at 2 months of age (*see* Figure E2C).

To model human emphysema, we chronically exposed *Fam13a*$^{-/-}$ mice and *Fam13a*$^{+/+}$ mice to CS or room air (air) for 6 months. Airspace size was assessed in four groups of mice. As previously reported (31), CS-exposed wild-type C57BL/6 *Fam13a*$^{+/+}$ mice developed significant although moderate airspace enlargement (15% increase) (Figures 1B and 1C; $P < 0.05$). However, *Fam13a*$^{-/-}$ mice were resistant to CS-induced emphysema and had similar distal airspace size as air-exposed *Fam13a*$^{-/-}$ mice, suggesting that the loss of *Fam13a* conferred resistance to CS-induced emphysema in murine lungs. Interestingly, CS exposure led to a trend, although insignificant, toward reduced levels of *Fam13a* mRNA in murine lungs (*see* Figure E3B). When respiratory mechanics were assessed, *Fam13a*$^{-/-}$ mice showed no differences in their lung compliance and pressure-volume loops compared with those obtained on *Fam13a*$^{+/+}$ mice when either exposed to air or CS for 6 months (*see* Figure E3C), consistent with the mild emphysema that develops in C57BL/6 mice when exposed to CS chronically (32).

CS-induced chronic lung inflammation is a crucial determinant of emphysema development (33–36). Proteinases and proinflammatory mediators released by CS-activated lung leukocytes and epithelial cells can also amplify lung inflammation and destruction (37–40). Therefore, we compared lung inflammatory responses in *Fam13a*$^{-/-}$ and *Fam13a*$^{+/+}$ mice exposed to CS for 1 month. Total leukocyte counts increased in bronchial alveolar lavage (BAL) samples after CS exposure, but no significant difference was observed in CS-exposed *Fam13a*$^{-/-}$ and *Fam13a*$^{+/+}$ mice (Figure 1D). This suggested that FAM13A promotes emphysema development without significantly altering the lung inflammatory response to CS.

FAM13A Interacts with Protein Phosphatase 2A and β-Catenin and Also Negatively Regulates β-Catenin Protein Stability

To identify signaling pathways related to FAM13A, we performed affinity purification followed by mass spectrometry in HEK293 cells transfected with FLAG/MYC–tagged human FAM13A (Figure 2A) to assess the full spectrum of cellular interacting partners of FAM13A. Among the identified FAM13A-interacting proteins, 11 proteins consisted of different subunits of Protein Phosphatase 2A (PP2A). Pathway analysis on FAM13A interacting proteins revealed enrichment for the "β-catenin phosphorylation cascade" and "degradation of β-catenin by the destruction complex" pathways (corrected $P < 0.01$ by Reactome pathway analysis). These results suggested that FAM13A may regulate PP2A-mediated β-catenin degradation. Because the β-catenin/Wnt pathway was previously shown to be essential for

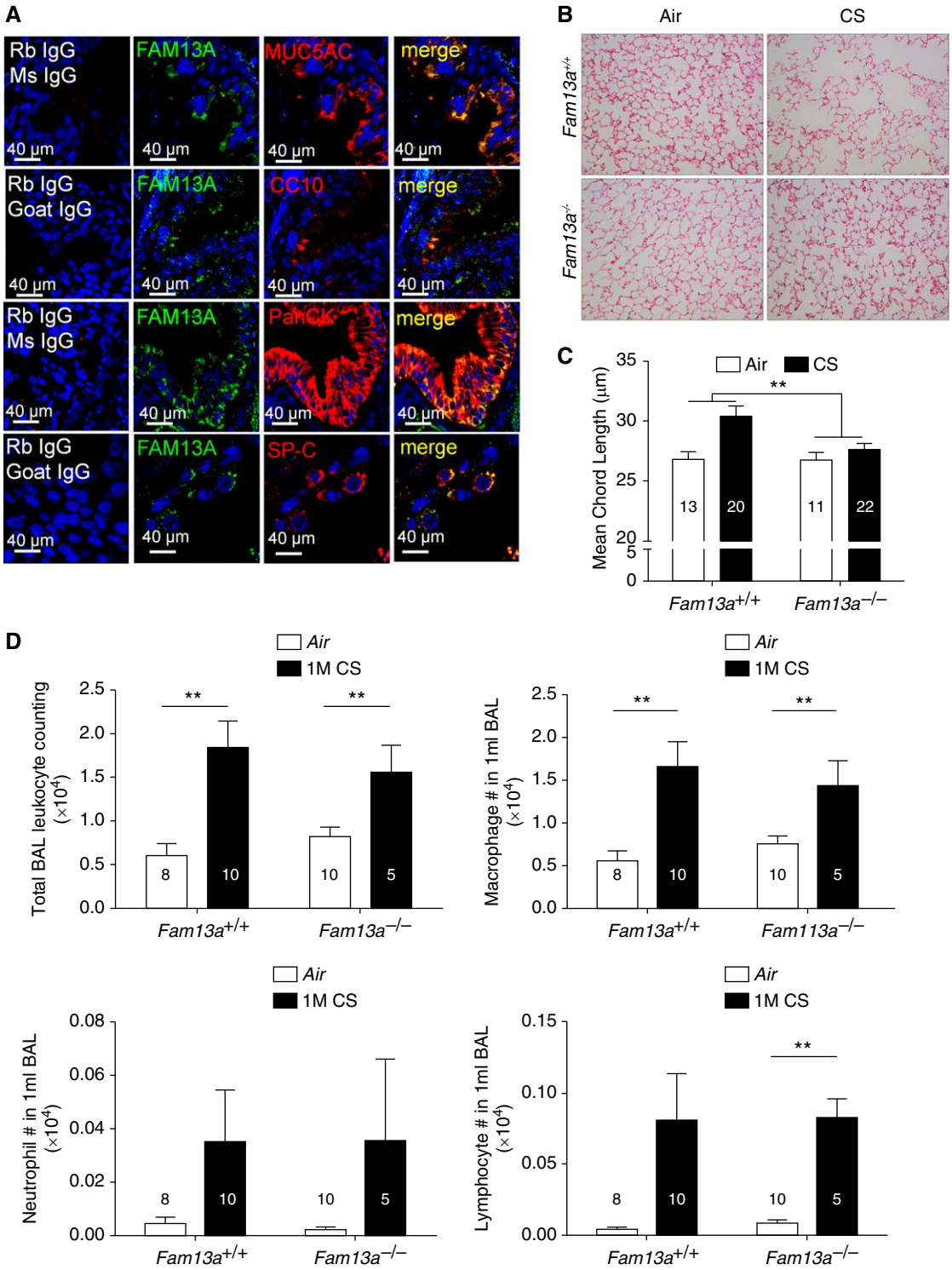

Figure 1. Depletion of *Fam13a* confers resistance to emphysema development in murine models. (*A*) FAM13A is localized in human airway cells including mucosal cells (MUC5AC), Club cells (CC10), pan-cytokeratin (PanCK, airway epithelial cells), and alveolar cells positive for surfactant protein-C (SP-C, alveolar type II cells). Representative images are from patients with very severe chronic obstructive pulmonary disease (n = 3) (FEV_1 <40%). Goat = anti-goat; Ms = anti-mouse; Rb = anti-rabbit. (*B*) Representative hematoxylin and eosin staining images (200×) in *Fam13a* null mice (*Fam13a*$^{-/-}$) and wild-type littermate control mice (*Fam13a*$^{+/+}$) exposed to cigarette smoke (CS) or room air (Air) for 6 months. (*C*) Mean alveolar chord length measurement in four groups of mice. Data shown are means ± SEM derived from 11–22 mice per group (the number of mice studied in each group is indicated inside each *column*). (*D*) Total leukocytes and leukocyte subsets in bronchoalveolar lavage (BAL) samples from *Fam13a*$^{-/-}$ and *Fam13a*$^{+/+}$ mice exposed to CS or air for 1 month. Two-way analysis of variance tests were used to analyze the effects of treatment and genotype in (*C*) and (*D*). Unpaired Student's *t* test, $^{**}P < 0.01$.

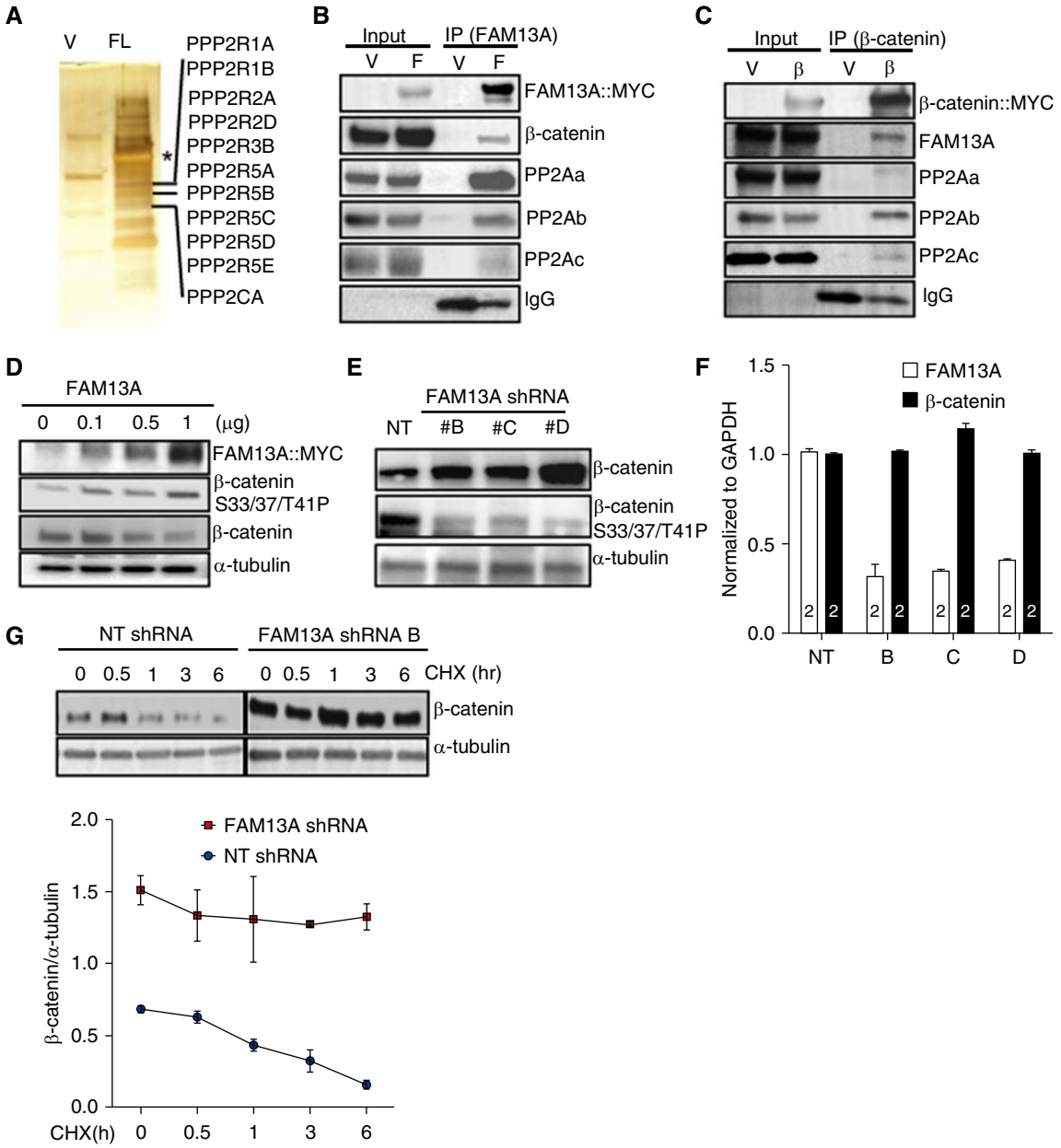

Figure 2. FAM13A interacts with PP2A/β-catenin complex and promotes degradation of β-catenin. (*A*) Affinity purification of cellular protein complexes associated with Flag-tagged FAM13A (FL) in HEK 293 cells as revealed by silver staining. Vector-transfected cells (V) were used as a control. The * indicates Flag-tagged FAM13A. Immunoprecipitation (IP) of FAM13A (*B*) and reverse immunoprecipitation (IP) targeting β-catenin (short for β) (*C*) was performed in HEK 293 cells. Examination of the levels and phosphorylation of β-catenin in human bronchial epithelial (16HBE) cells transfected with either increasing amount of FAM13A (*D*) or short hairpin RNAs (shRNAs) targeting FAM13A (*E*). NT = nontarget control hairpins; columns B, C, and D = three independent hairpins targeting FAM13A. (*F*) Expression of FAM13A and β-catenin in cells measured by reverse transcriptase–polymerase chain reaction. Glyceraldehyde 3-phosphate dehydrogenase (GAPDH) was used as a reference gene. (*G*) Half-life of β-catenin was measured in 16HBE cells stably infected with nontargeting control shRNA (NT) or *FAM13A* shRNA B and treated with cycloheximide (CHX, 5 nM) for various time periods. Means ± SD were from two independent repeats normalized to α-tubulin. Linear mixed effects model was used to compare differences in slope of β-catenin reductions in NT-shRNA and FAM13A shRNA–transfected cells ($P < 0.01$).

COPD/emphysema development (21), we decided to focus our investigation on this pathway. Additional pathways enriched in FAM13A interacting proteins are listed in Table E1.

PP2A is a heterotrimeric substrate-specific serine/threonine protein phosphatase, consisting of a catalytic subunit (PP2Ac), a structural subunit (PP2Aa), and a variable regulatory subunit (PP2Ab). The association of the PP2Ab subunit with different adaptor proteins facilitates recognition of specific substrates by PP2A (41). As a known substrate of PP2A, β-catenin prevented experimental

emphysema development in a murine model (21). Therefore, we tested the hypothesis that FAM13A recruits PP2A and thus regulates the stability of β-catenin. Immunoprecipitation targeting FLAG-tagged FAM13A pulled down PP2A and β-catenin (Figure 2B). Of note, FAM13A robustly coimmunoprecipitated with the structural PP2Aa subunit and the regulatory PP2Ab subunit, but showed weak interaction with its catalytic subunit (PP2Ac). Also, β-catenin coimmunoprecipitated with FAM13A, PP2Ab, and PP2Ac (Figure 2C), suggesting that FAM13A-PP2Ab-β-catenin form one protein complex.

We then tested whether FAM13A regulates β-catenin levels in airway epithelial cells. In the HBE cell line, 16HBE cells, the overexpression of FLAG-tagged human FAM13A increased phosphorylation of β-catenin but decreased total β-catenin protein levels (Figure 2D), whereas silencing of *FAM13A* led to reduced phosphorylation of β-catenin but increased total cellular β-catenin protein levels (Figure 2E) without altering its mRNA levels (Figure 2F). Consistent with these results, silencing of *FAM13A* extended the half-life of the β-catenin protein in 16HBE cells (Figure 2G). Similarly, the half-life of β-catenin was also extended in alveolar epithelial cells from *Fam13a*$^{-/-}$ mice compared with those from *Fam13a*$^{+/+}$ mice (*see* Figure E4A). Our findings support that endogenous human FAM13A coprecipitates with the PP2A and β-catenin complex and promotes phosphorylation and degradation of β-catenin. This is inconsistent with findings from a recent study showing that overexpressing murine *Fam13a* promotes degradation of Axin 1 thus leading to accumulation of β-catenin in A549 cells. Therefore, we assessed Axin 1 levels in 16HBE cells in which human FAM13A was overexpressed or silenced. No significant changes in Axin 1 protein levels were detected (*see* Figure E4B). This result was also confirmed in alveolar epithelial cells from *Fam13a*$^{-/-}$ mice (*see* Figure E4C). Thus, regulation of Axin 1 protein levels by FAM13A may be cell type specific.

β-catenin is normally sequestered in membrane through binding with E-cadherin, and thus is protected from degradation by its degradation complex. However, under *FAM13A* deficiency, enhanced interaction between β-catenin and E-cadherin was detected (*see* Figure E5A), indicating that FAM13A might disassociate β-catenin from the E-cadherin/β-catenin complex. Thus, overexpression of FAM13A led to reduced levels of membrane-bound β-catenin (*see* Figure E5B). However, CS extract treatment disrupted the cytoplasmic interaction between FAM13A and β-catenin in 16HBE cells (*see* Figure E5A), suggesting a dynamic interaction between FAM13A and β-catenin.

FAM13A Regulates β-Catenin Activity and Promotes Cell Proliferation

Accumulated β-catenin molecules can translocate into the cell nucleus where they bind to the TCF4/LEF transcription factor to activate the canonical Wnt pathway (42, 43). To identify the mechanism by which FAM13A promotes degradation of β-catenin and shed light on the composition of the FAM13A/PP2Ab/β-catenin complex, we applied the TOPFLASH reporter assay in 16HBE cells to monitor transcriptional activity of β-catenin regulated by FAM13A (Figure 3A). Cells transfected with constitutively active mutant β-catenin (β-catenin::CS2) (44) were used as positive controls and cells treated with an inhibitor of β-catenin, PKF118-310 (7.5 μg/ml), were used as negative controls in this assay. In 16HBE cells, depletion of FAM13A led to an approximately threefold increase in luciferase activity, and this effect was attenuated by overexpression of FAM13A (Figure 3A), suggesting that FAM13A regulates the activity of the Wnt pathway. Activation of the Wnt pathway can increase

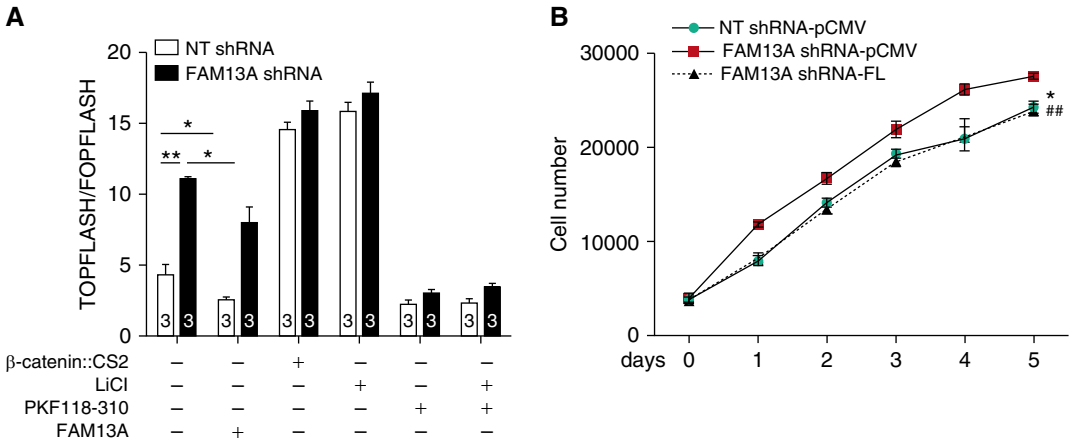

Figure 3. FAM13A down-regulates β-catenin activity and regulates cell proliferation. (*A*) Assessments of the β-catenin activity by TOPFLASH reporter assay in human bronchial epithelial (16HBE) cells transfected with full-length human *FAM13A*. Cells treated with β-catenin inhibitor PKF118-310 (7.5 μg/ml) overnight were used as negative controls and cells transfected with constitutively active β-catenin mutant (β-catenin::CS2) as positive controls in this reporter assay. Statistical comparisons in controls were not shown. Means ± SD were from triplicate assays with separately transfected and treated wells per condition. *$P <$ 0.05, **$P < 0.01$. Unpaired Student's *t* test was applied. One representative repeat from three independent biologic repeats was shown here. The other two repeats were shown in Figure E4D. (*B*) Cell growth curve in 16HBE cells transfected with different constructs. Z-test was used to compare the slopes between the curves using linear regression model. The significance was indicated right to the last time point of each curve: *Comparison between FAM13A shRNA-pCMV and NT shRNA-pCMV, $P < 0.05$; ##Comparison between FAM13A shRNA-pCMV and FAM13A shRNA-FL, $P < 0.05$. FL = full-length FAM13A; NT shRNA = nontargeting shRNA; pCMV = empty vector as controls; shRNA = short hairpin RNA.

cell proliferation (45) and modulate lung injury/repair responses during CS-induced emphysema development (21). Consistent with this paradigm, silencing of *FAM13A* increased cell proliferation in 16HBE cells, which was reversed by transfection of *FAM13A* (Figure 3B), suggesting that FAM13A regulates cell proliferation.

FAM13A Facilitates the Interaction between PP2A and β-Catenin, Thus Promoting β-Catenin Degradation

Because FAM13A forms a complex with both PP2A and β-catenin, we next asked whether this interaction contributes to the regulation of FAM13A on the protein stability of β-catenin. Degradation of β-catenin relies on the activation of the kinase GSK-3β, which can be achieved through dephosphorylation of GSK-3β at Ser 9 by PP2A. Therefore, we assessed PP2A phosphatase activity in the PP2A/β-catenin /GSK-3β complex regulated by FAM13A. Interestingly, although total cellular PP2A catalytic activity remained intact in 16HBE cells depleted of *FAM13A* (Figure 4A), we observed significantly reduced phosphatase activity of PP2Ac in the β-catenin protein complex (Figure 4B). Furthermore, Western blotting on the immunoprecipitated complex demonstrated reductions in the amount of PP2Ab and PP2Ac associated with the β-catenin complex in the absence of FAM13A (Figures 4C and 4D). These results suggest that FAM13A may facilitate the binding between PP2Ab and β-catenin/GSK-3β, which dephosphorylates and activates GSK-3β that promotes degradation of β-catenin (Figure 4E).

Increased β-Catenin Signaling in *Fam13a*$^{-/-}$ Mice

We further assessed β-catenin signaling changes and cell proliferation that may contribute to the resistance of *Fam13a*$^{-/-}$ mice to CS-induced emphysema using lungs from *Fam13a*$^{-/-}$ mice exposed to CS for 1 or 6 months. First, in line with the previously mentioned *in vitro* model, we detected decreased β-catenin S33/37/T41 phosphorylation (S33/37/T41P), increased β-catenin levels, and increased GSK-3β S9 phosphorylation in whole lung samples from *Fam13a*$^{-/-}$ mice compared with *Fam13a*$^{+/+}$ mice (Figure 5A; *see* Figures E6A and E7). Expression levels of known target genes of β-catenin, TCF7 (46) and WISP2 (47), were significantly increased in

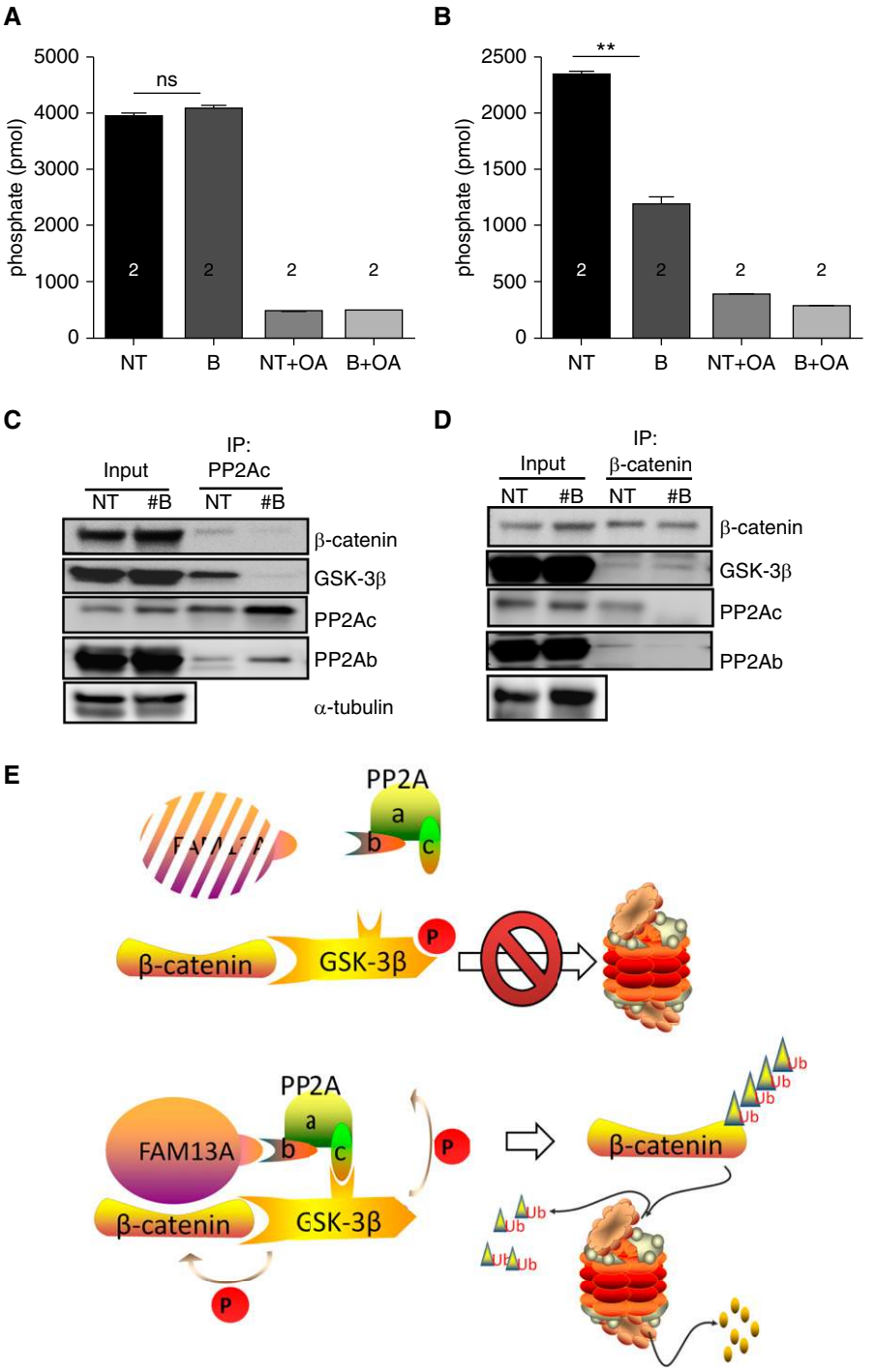

Figure 4. FAM13A is required for the interaction between β-catenin, and PP2A thus promotes degradation of β-catenin. (*A* and *B*) Phosphatase activity of PP2A in 16HBE cells stably infected with nontargeting control shRNA (NT) or *FAM13A* shRNA B (B) was measured using PP2A Immunoprecipitation Phosphatase Assay Kit (Millipore). Cells treated with okadaic acid (OA) for 18 hours were used as negative controls in this assay. Cellular proteins were immunoprecipitated with PP2Ac antibody (*A*) or β-catenin antibody (*B*) separately. Note that the same amount of cellular proteins was used for immunoprecipitation (IP) in NT cells as in B cells. (*C*) Detection of β-catenin and PP2Ab associated with PP2Ac in NT cells and B cells. (*D*) Detection of PP2Ac and PP2Ab associated with β-catenin in NT cells and B cells. $^{**}P < 0.05$. Unpaired Student's *t* test was applied. (*E*) Schematic illustration on how FAM13A regulates β-catenin protein stability through interacting with PP2A. 16HBE = human bronchial epithelial cells; GSK-3β = glycogen synthase kinase 3β; ns = not significant; shRNA = short hairpin RNA.

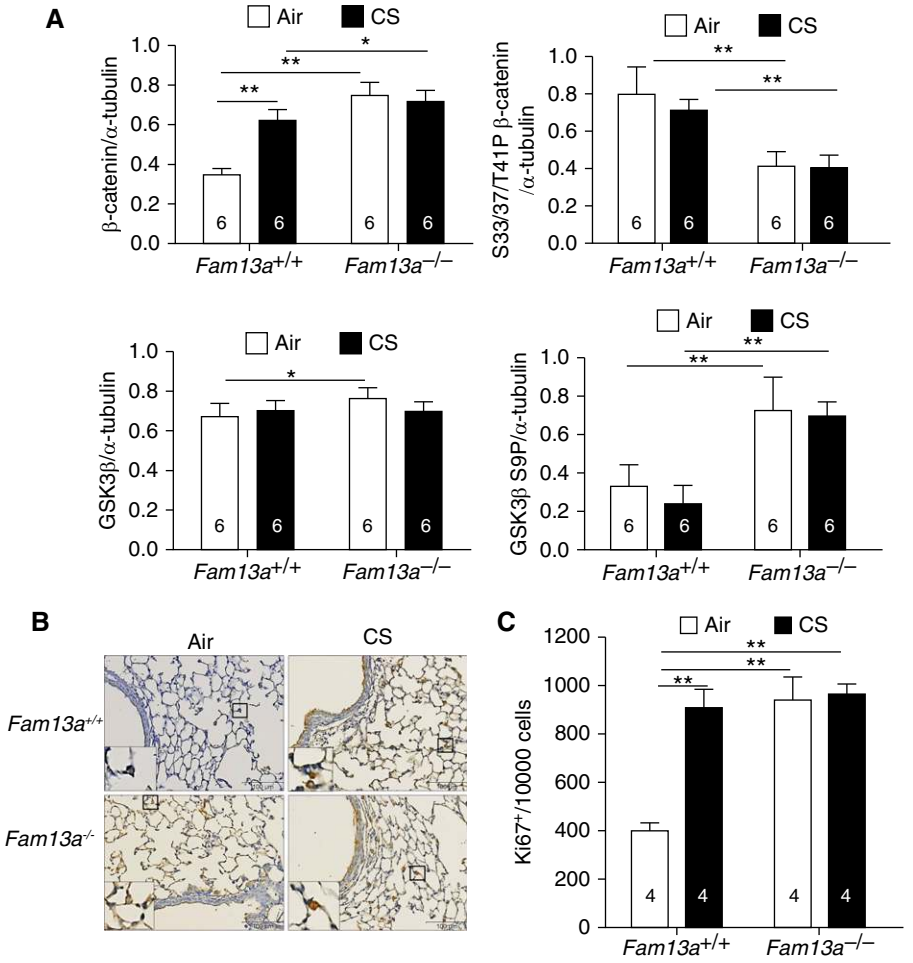

Figure 5. Depletion of *Fam13a* leads to activation of β-catenin signaling in murine lungs. (*A*) Quantification of total and phosphorylated β-catenin and GSK-3β by Western blotting in murine lungs from the same groups of mice exposed to air or cigarette smoke (CS) for 6 months as in Figure 6A. Representative Ki67 staining images (200× magnification with 600× magnification in *insets*) (*B*) and quantifications (*C*) in lung sections from *Fam13a*$^{-/-}$ and *Fam13a*$^{+/+}$ mice exposed to air or cigarette smoke for 6 months. Cells positive for Ki67 staining were counted in six randomly acquired fields per mouse. Data are mean ± SEM from four mice per group (number of mice in each group is indicated inside each *column*). *$P < 0.05$; **$P < 0.01$, unpaired Student's *t* test analysis in *A* and *C*. GSK3β = glycogen synthase kinase 3β.

lung samples from *Fam13a*$^{-/-}$ mice compared with *Fam13a*$^{+/+}$ mice (*see* Figure E6B). However, CS exposure also showed genotype-dependent regulation on expression of these two genes. Taken together, these results indicate that loss of Fam13a results in activation of β-catenin signaling.

We also assessed cell proliferation in murine lung sections by staining them with Ki67. There was increased staining for Ki67 in the lungs of *Fam13a*$^{-/-}$ mice compared with *Fam13a*$^{+/+}$ mice exposed to air for 6 months (Figures 5B and 5C). CS induced increases in Ki67 staining in *Fam13a*$^{+/+}$ lungs, mainly in alveolar septal cells. However, Ki67 staining did not increase further in alveolar septal cells in CS- versus air-exposed *Fam13a*$^{-/-}$ mice (Figures 5B and 5C). We hypothesize that *Fam13a*$^{+/+}$ mice develop a compensatory response in the lung to CS exposure (Figures 5B and 5C). This notion is supported by the protective role of β-catenin activation in the elastase-induced emphysema model (21). Taken together, these results indicate that loss of *Fam13a* resulted in activation of β-catenin signaling and increased cell proliferation (Figures 5B and 5C).

FAM13A Determines Susceptibility to Emphysema by Regulating β-Catenin Signaling

Next, we directly tested the hypothesis that activation of β-catenin is required to protect *Fam13a*$^{-/-}$ mice from developing emphysema by evaluating the effects of a β-catenin inhibitor in *Fam13a*$^{+/+}$ versus *Fam13a*$^{-/-}$ mice with emphysema. We used a porcine pancreatic elastase (PPE)-induced emphysema murine model to test this hypothesis because β-catenin has been shown to protect mice from elastase-induced emphysema (21); and the β-catenin transcriptional inhibitor we studied (PKF118-310) produces hepatic toxicity, which precludes its use in chronic model systems, such as the 6-month CS exposure model of emphysema. We coadministered PKF118-310 (48, 49) and PPE to *Fam13a*$^{+/+}$ and *Fam13a*$^{-/-}$ mice and measured emphysema development (50). The optimal dose of PKF118-310 (0.25 mg/kg) tested was chosen based on the significant inhibition of *Axin2* expression associated with minimal liver toxicity after acute administration (*see* Figures E8A–E8C).

PPE treatment of mice did not induce significant changes in *Fam13a* expression in lungs (*see* Figure E9A). PKF118-130 treatment alone did not affect distal airspace size (*see* Figures E9B–E9C). Similar to the protective effect of loss of *Fam13a* in CS-exposed mice, PPE-treated *Fam13a*$^{-/-}$ mice developed minimal airspace enlargement, but this protection was reversed by coadministration of PKF118-310 (Figures 6A and 6B). Furthermore, treating *Fam13a*$^{+/+}$ mice with PPE reduced Ki67 staining in alveolar septal cells (Figure 6C), likely reflecting the acute and destructive effects of PPE on the lung, in contrast to the milder effects of chronic CS exposure on the lung (51, 52). Interestingly, coadministration of PPE and PKF118-310 to *Fam13a*$^{-/-}$ mice reduced Ki67 staining in *Fam13a*$^{-/-}$ lungs. These results suggest that increased alveolar septal cell proliferation in *Fam13a*$^{-/-}$ mice relies on activation of β-catenin, which may contribute to reduced emphysema development. These data also further supported a protective role for β-catenin in emphysema development (21).

BAL leukocytes increased to a similar extent in PPE-treated *Fam13a*$^{+/+}$ and *Fam13a*$^{-/-}$ mice. Coadministration of PPE and PKF118-310 reduced BAL leukocyte counts only modestly in *Fam13a*$^{+/+}$ mice but had no effects on BAL leukocyte counts in *Fam13a*$^{-/-}$ mice (Figure 6D). These

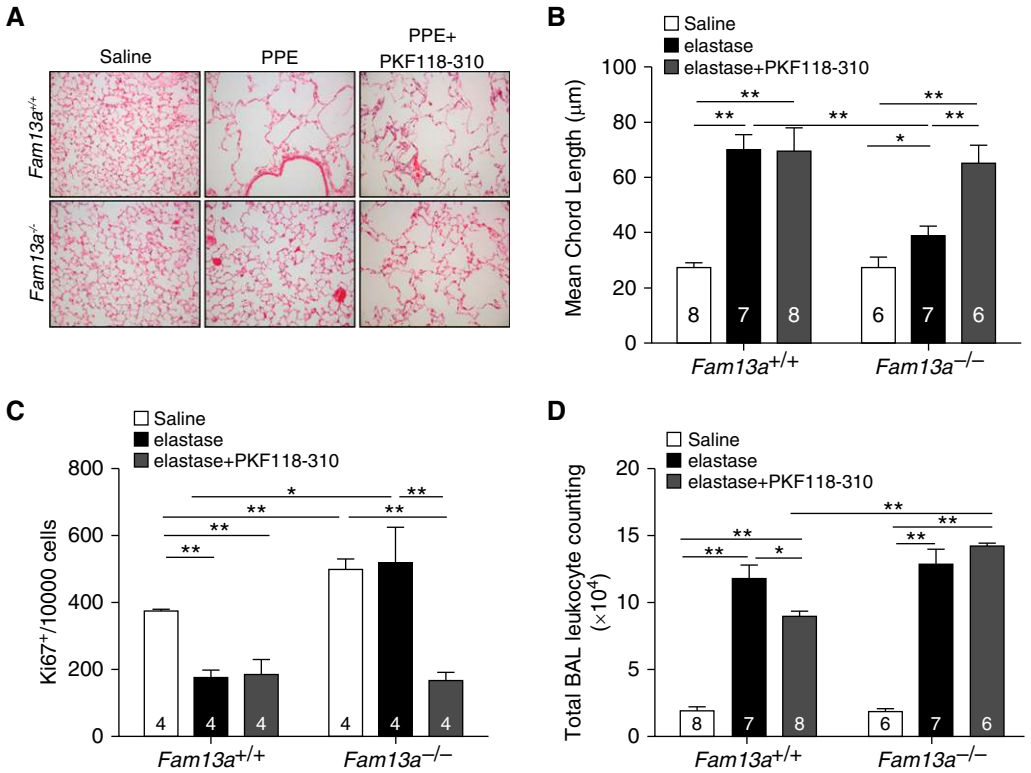

Figure 6. Inhibition on transcriptional activity of β-catenin reverted the resistance to emphysema in *Fam13a*$^{-/-}$ mice in elastase-induced experimental emphysema. (*A*) Airspace size assessment in *Fam13a*$^{+/+}$ and *Fam13a*$^{-/-}$ mice treated with phosphate-buffered saline, porcine pancreatic elastase (PPE), or β-catenin inhibitor PKF118-310 (200× magnification). (*B*) Mean chord length was quantified on randomly selected images in a blinded fashion. Data shown are means ± SEM derived from n = 6–8 mice per group (number in each *column* represents the number of mice in each group). (*C*) Ki67 staining measurement in lung tissue from mice treated with PPE. Data shown are mean ± SEM from four mice per group with six randomly acquired images of lung sections stained for Ki67. (*D*) Total leukocytes counted in bronchoalveolar lavage (BAL) samples from *Fam13a*$^{-/-}$ and *Fam13a*$^{+/+}$ mice treated with PPE with or without PKF118-310. $^{*}P < 0.05$; $^{**}P < 0.01$, unpaired Student's *t* test in *B–D*.

results suggest that Fam13a-regulated β-catenin signaling does not play a major role in regulating the inflammatory response in the PPE-induced emphysema model.

Decreased β-Catenin and Increased FAM13A Protein Levels in Human COPD Lungs

Next, we measured FAM13A protein levels in lungs from subjects with COPD and healthy ex-smokers (control subjects) by Western blotting. Increased FAM13A and reduced β-catenin protein levels were detected in very severe COPD lungs (Global Initiative for Chronic Obstructive Lung Disease stage IV) compared with control lungs (Figures 7A and 7B; *see* Figure E10), consistent with a previous report that the Wnt signaling pathway is reduced in human COPD lungs (53). However, no significant changes were detected in *FAM13A* or *CTNNB1* mRNA levels (Figures 7C and 7D). These findings in human lung samples indicate that increased FAM13A (Figure 7A) and decreased β-catenin protein levels (Figure 7B) are associated with very severe COPD. These patients may have impaired lung repair that could contribute to their increased risk of emphysema development with CS exposure.

Discussion

GWASs have demonstrated a consistent association with COPD susceptibility at the *FAM13A* locus. However, GWAS alone is unable to address whether the *FAM13A* gene is protective or whether it accelerates COPD development, or even if *FAM13A* is the key gene at that GWAS locus. Herein, we demonstrated that *Fam13a* null mice (*Fam13a*$^{-/-}$) were resistant to chronic CS or elastase-induced emphysema development. FAM13A also promotes the assembly of the PP2Ab/β-catenin complex leading to degradation of β-catenin. It is noteworthy that activation of β-catenin signaling contributes to airway (18) and alveolar (21, 54) epithelial repair/regeneration after various injuries. Hence, we connect *FAM13A*, located in one of the most consistently associated COPD GWAS regions, with β-catenin signaling, a potentially important repair pathway that determines COPD development and/or progression.

Pathologic changes in human COPD lungs include emphysema (destruction of alveolar walls and reduced alveolar surface areas), small airway remodeling (mainly composed of small airway fibrosis and destruction), and chronic bronchitis. Herein, we focused on emphysema development that may result from a combination of increased vulnerability to CS-induced injury in alveolar epithelial cells and failure to adequately repair. Our results demonstrate that *Fam13a* does not regulate the lung inflammatory response to

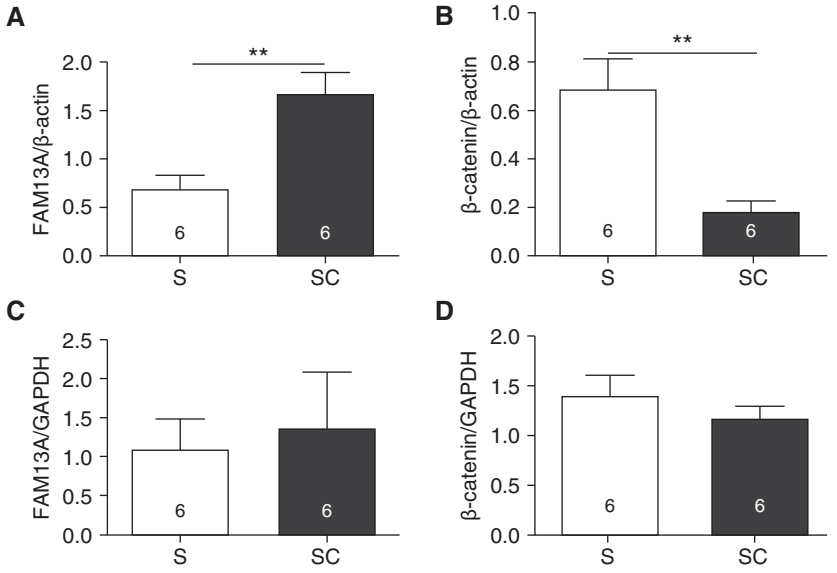

Figure 7. Increased FAM13A levels and reduced β-catenin levels are associated with human emphysema. (*A*) Increased levels of FAM13A protein and decreased levels of β-catenin protein (*B*) in human chronic obstructive pulmonary disease lungs compared with healthy ex-smokers. Data shown are mean ± SEM from six subjects for each group. $^{**}P < 0.01$, unpaired Student's *t* tests were used to analyze the data. (*C* and *D*) Measurements on *FAM13A* (*C*) and β-catenin (*D*) mRNA levels in human chronic obstructive pulmonary disease lungs by reverse transcriptase polymerase chain reaction. GAPDH = glyceraldehyde 3-phosphate dehydrogenase; S = healthy ex-smokers; SC = very severe COPD.

either CS or PPE. Rather, our data support the notion that the resistance of *Fam13a*$^{-/-}$ mice to PPE-induced airspace enlargement is likely caused (at least in part) by more efficient lung repair in *Fam13a*$^{-/-}$ mice, possibly because of accumulation of β-catenin in alveolar epithelial cells (*see* Figure E4A), enhanced β-catenin signaling in lungs (*see* Figures E6 and E7), and increased cell proliferation (Figure 6C) in the absence of *Fam13a*.

Different types of epithelial cells in the respiratory tract may have similar or different responses to CS, which lead to destruction of the alveolar walls and/or abnormal repair processes in the small airways associated with deposition of extracellular matrix. Therefore, the molecular mechanisms by which FAM13A contributes to COPD pathogenesis identified in HBE cells (16HBE cells) were also assessed and confirmed *in vivo* using lung samples (Figures 5 and 6) with experimental emphysema and primary alveolar epithelial cells (*see* Figure E4A) from *Fam13a*$^{+/+}$ and *Fam13a*$^{-/-}$ mice. *Fam13a*$^{-/-}$ mice were protected from PPE-induced emphysema. This protection was reversed by treating *Fam13a*$^{-/-}$ mice with a β-catenin inhibitor, which led to reduced alveolar septal cell proliferation in *Fam13a*$^{-/-}$ mice that were treated with PPE and the β-catenin inhibitor (Figure 6C), suggesting that β-catenin activation is required for Fam13a-regulated cell proliferation and reduced emphysema susceptibility in *Fam13a*$^{-/-}$ mice.

Using murine models to recapitulate human COPD pathologic changes has been challenging because of anatomic and physiologic differences between humans and mice. The chronic CS exposure model produces relatively mild emphysema (with only ~15% increases in airspace size), but it is still so far the best approximation to human COPD because it uses the same environmental risk factor, and induces lung inflammation and airspace enlargement by broadly similar mechanisms as those that contribute to human COPD (52). The elastase-induced emphysema model is an acute emphysema model. Although it lacks a number of the pathologic features of human COPD, the elastase model is an efficient way to test various preventative and therapeutic strategies for emphysema (51). Therefore, the approach to use both models herein enabled us to gain a more comprehensive picture of the mechanisms by which FAM13A promotes susceptibility to emphysema development through regulating β-catenin activity.

The lung inflammatory response in *Fam13a*$^{-/-}$ mice to 1 month of CS exposure was similar to that of *Fam13a*$^{+/+}$ mice. Although activation of β-catenin signaling was shown to repress the inflammatory response of alveolar epithelial cells through TLR signaling *in vitro* (55), conditional depletion of β-catenin in AT II cells did not significantly alter lung inflammatory responses to bleomycin (56), similar to our results in CS- or elastase-treated *Fam13a*$^{-/-}$ mice (Figure 6D). Therefore, it is more likely that enhanced epithelial repair caused by activation of β-catenin signaling in *Fam13a*$^{-/-}$ mice contributed to their resistance to CS-induced emphysema. However, it is noteworthy that chronic CS exposure in *Fam13a*$^{+/+}$ mice increased cell proliferation, whereas acute instillation of PPE reduced cell proliferation in *Fam13a*$^{+/+}$ murine lungs but not in *Fam13a*$^{-/-}$ mice (Figure 6C). These results indicate differences in the mechanisms, severity, and/or duration, of injury in these two emphysema models. Chronic CS exposure over 6 months induces a milder and less acute form of airspace enlargement associated with a less intense inflammatory and injury response in the lung. Also, low concentrations of CS extract increased cell proliferation *in vitro* (57, 58), consistent with our findings *in vivo*. However, PPE potently degrades lung extracellular matrix proteins that are crucial for the survival of lung structural cells, thus leading to reduced cell proliferation as reported previously (59, 60). Therefore, it was not entirely surprising that PPE treatment in mice reduced cell proliferation.

The FAM13A interacting partner PP2A is one major Ser/Thr phosphatase in mammalian cells that forms stable complexes with a large number of regulatory subunits. Different regulatory b subunits of PP2A determine the substrate specificity of PP2A, which regulates a variety of cell biologic processes and signaling pathways, including mitosis, apoptosis, and DNA damage signaling (reviewed in Reference 61). Importantly, these regulatory subunits also regulate Akt, Wnt, and c-Myc signaling by interacting with different adaptor proteins. Our data suggested that FAM13A may facilitate recruitment of PP2Ab and β-catenin and promote degradation of β-catenin, consistent with the inhibition of

PP2Ab on the Wnt pathway in *Xenopus* (62) possibly by promoting degradation of β-catenin (63). Given that there are four families of PP2Ab subunits encoded by 15 human genes (reviewed in Reference 62), additional studies are needed to identify which subunits of PP2Ab are recruited by FAM13A to the β-catenin degradation complex. Nevertheless, our studies linked PP2A to human COPD by FAM13A promoting degradation of β-catenin. Another report also linked PP2A to COPD by showing increased activity of PP2A in murine lungs exposed to CS for 3 days (64). When the expression of FAM13A is silenced in 16HBE cells, we detected reductions in PP2A activity only in β-catenin-associated PP2A (Figures 4A and 4B). The overall contributions of PP2A activity induced by CS to emphysema development need further investigation.

Another group recently showed that overexpression of murine FAM13A interacts with PP2Ab, which regulated the translocation of FAM13A from the nucleus to the cytoplasm (65). However, in either murine/human lung sections (Figure 1; *see* Figure E1) or in 16HBE cells transfected with tagged human FAM13A, we found little if any FAM13A in the nucleus (*see* Figures E11A and E11B). Therefore, further investigations are warranted to assess the biologic function of nuclear FAM13A under physiologic and pathologic conditions. In contrast, it was also reported that overexpression of myc-tagged murine FAM13A increased protein levels of exogenous myc-tagged β-catenin in A549 cells (65), a human lung adenocarcinoma cell line. This was attributed to reduced protein levels of Axin1, a key molecule in the β-catenin degradation complex. However, we detected no accumulation of *AXIN1* in *FAM13A*-deficient human 16HBE cells or primary alveolar epithelial cells isolated from *Fam13a*$^{-/-}$ mice. The discrepancy in the results in our study versus the prior report could be explained by use of different cell lines, and also by gain-of-function approaches (overexpression of murine protein in human cells) in the prior report versus loss-of-function approaches in our study. Future studies will address whether there is dynamic and complex regulation of β-catenin by FAM13A under different pathologic conditions, such as lung cancer and COPD.

Cellular levels of β-catenin are tightly controlled by its destruction complex including the crucial kinase GSK-3β that phosphorylates β-catenin for proteasome-dependent degradation. Although GSK-3β Ser9 phosphorylation was shown to be dispensable for Wnt3a-mediated β-catenin accumulation in HEK 293 cells (66), several other independent studies have challenged this conclusion using various models (67, 68). The Ser9 site of GSK-3β is a well-accepted target for PP2A. We observed increased Ser9 phosphorylation accompanied by accumulation of β-catenin in the absence of FAM13A *in vivo*, suggesting that GSK-3β Ser9 phosphorylation correlates with FAM13A-regulated β-catenin degradation. In contrast, a transient increase of GSK-3B Ser9 was detected in murine lungs after 1 month of CS exposure (*see* Figure E7), but no significant increases were detected after 6 months of CS exposure. These results indicate that CS-induced rapid inactivation of GSK-3β through Ser9 phosphorylation may contribute to increases in β-catenin level after acute CS exposure.

Activation of β-catenin signaling has been reported to contribute to the repair/regeneration processes triggered by lung injury in adulthood (69). Stabilized β-catenin molecules translocate to the nucleus, where they activate the expression of Wnt target genes that promote cell proliferation (15–17) and limit cell differentiation (16, 18). Therefore, activation of β-catenin signaling contributes to both airway (18, 19) and alveolar epithelial cell repair (20–22) after various injuries (18, 19, 21, 56). Our data suggest that reduced levels of FAM13A may promote lung repair by enhancing β-catenin signaling in CS-exposed or PPE-treated lungs to promote epithelial proliferation and thereby limit emphysema development.

Compared with ex-smoker control lungs, we found that β-catenin protein levels were significantly reduced in COPD lungs in contrast to a previous report showing similar β-catenin mRNA and protein levels in COPD and control lungs (21). There are several possibilities that could contribute to such discordant results. First, previous measurements of β-catenin levels in COPD lungs were performed using rejected transplant donor lungs as controls, whereas we used lungs from ex-smokers with normal lung function as controls. Second, the COPD lungs were obtained from different sources in these two studies. We included a small number of lung tissue samples obtained in subjects that were characterized through the LTRC. COPD is a heterogeneous disease, and patients have varying combinations of emphysema, and large and small airway disease. It is not clear which of these COPD phenotypes were included in either study because chest computed tomography scan analyses were unavailable on these subjects. In addition, the COPD cases in our study had very severe COPD at a relatively early age. Thus, studying patients with different COPD phenotypes could explain, in part, the differences between these two studies.

In human lungs, expression quantitative trait locus analysis suggested that COPD risk alleles at the *FAM13A* locus may be associated with increased expression of *FAM13A* (70), which could potentially lead to a more effective lung repair program in lung alveolar epithelial cells after CS exposure. Importantly, FAM13A protein levels are increased and β-catenin protein levels are decreased in human COPD lung tissues compared with ex-smokers without COPD, suggesting that FAM13A possibly promotes the development of human and murine emphysema by inhibiting the β-catenin-mediated lung repair pathway. Admittedly, the impact of functional variants for human complex diseases on gene expression is likely more moderate than complete depletion of genes in murine knockout models. We recognize this limitation due to differential perturbations on *FAM13A* gene expression in our post-GWAS functional assessment. However, the knock-out mouse model is necessary and instrumental to elucidate biologic functions of FAM13A (and other genes implicated by GWAS) in the pathogenesis of COPD.

Further studies are warranted to identify the functional genetic variants at the *FAM13A* locus that influence COPD susceptibility and to determine their mechanism of action. The combination of the knock-out mouse model with functional variants identification will elucidate a complete mechanism by which genetic variations at the *FAM13A* locus determine the susceptibility to develop COPD. Genetic variants within the *FAM13A* region, although in a different part of this genomic region than the COPD GWAS variants (12), have also been associated with idiopathic pulmonary fibrosis (71). Thus, additional work is required to determine whether any of the pathways identified in

our COPD work are also relevant for interstitial lung disease.

In summary, our data provide *in vitro* and *in vivo* evidence to demonstrate activities for the FAM13A-PP2Ab-β-catenin axis in the development of human and murine emphysema and a molecular mechanism by which FAM13A possibly influences susceptibility to human COPD development. ■

Author disclosures are available with the text of this article at www.atsjournals.org.

Acknowledgment: The authors thank Lung Tissue Research Consortium, Dr. Bartolome Celli, Dr. Victor Pinto-Plata, and Dr. Ivan Rosas (Brigham and Women's Hospital, Boston, MA) for providing human lung tissue specimens for our analysis. They also thank Dr. Ningzhi Xu and Dr. Hongxia Zhu (Chinese Academy of Medical Sciences & Peking Union Medical College, P. R. China) for providing TOPFLASH and TK-rennila reporter plasmids. The authors also thank Dr. Xingbin Ai (Harvard Medical School, Boston, MA) for her generous gift of the constitutively active mutant β-catenin (β-catenin:CS2) construct.

References

1. Miniño AM. Death in the United States, 2011. *NCHS Data Brief* 2013; 115:1–8.
2. Miniño AM, Kochanek KD. Division of Vital Statistics. Deaths: preliminary data for 2008. U.S. Department of Health and Human Services Centers for Disease Control and Prevention, National Center for Health Statistics, National Vital Statistics System. National Vital Statistics Reports 2010:1–72.
3. Burrows B, Knudson RJ, Cline MG, Lebowitz MD. Quantitative relationships between cigarette smoking and ventilatory function. *Am Rev Respir Dis* 1977;115:195–205.
4. Fletcher C, Peto R, Tinker C, Speizer FE. Factors related to the development of airflow obstruction. In: The natural history of chronic bronchitis and emphysema. Oxford: Oxford University Press; 1976. pp. 70–105.
5. McCloskey SC, Patel BD, Hinchliffe SJ, Reid ED, Wareham NJ, Lomas DA. Siblings of patients with severe chronic obstructive pulmonary disease have a significant risk of airflow obstruction. *Am J Respir Crit Care Med* 2001;164:1419–1424.
6. Silverman EK, Chapman HA, Drazen JM, Weiss ST, Rosner B, Campbell EJ, O'Donnell WJ, Reilly JJ, Ginns L, Mentzer S, *et al*. Genetic epidemiology of severe, early-onset chronic obstructive pulmonary disease. Risk to relatives for airflow obstruction and chronic bronchitis. *Am J Respir Crit Care Med* 1998;157: 1770–1778.
7. Gibson G. Hints of hidden heritability in GWAS. *Nat Genet* 2010;42: 558–560.
8. Manolio TA. Genome-wide association studies and assessment of the risk of disease. *N Engl J Med* 2010;363:166–176.
9. Hindorff LA, Sethupathy P, Junkins HA, Ramos EM, Mehta JP, Collins FS, Manolio TA. Potential etiologic and functional implications of genome-wide association loci for human diseases and traits. *Proc Natl Acad Sci USA* 2009;106:9362–9367.
10. Lander ES. Initial impact of the sequencing of the human genome. *Nature* 2011;470:187–197.
11. Cho MH, Boutaoui N, Klanderman BJ, Sylvia JS, Ziniti JP, Hersh CP, DeMeo DL, Hunninghake GM, Litonjua AA, Sparrow D, *et al*. Variants in FAM13A are associated with chronic obstructive pulmonary disease. *Nat Genet* 2010;42:200–202.
12. Cho MH, McDonald ML, Zhou X, Mattheisen M, Castaldi PJ, Hersh CP, Demeo DL, Sylvia JS, Ziniti J, Laird NM, *et al*.; NETT Genetics, ICGN, ECLIPSE and COPDGene Investigators. Risk loci for chronic obstructive pulmonary disease: a genome-wide association study and meta-analysis. *Lancet Respir Med* 2014;2:214–225.
13. Baarsma HA, Spanjer AI, Haitsma G, Engelbertink LH, Meurs H, Jonker MR, Timens W, Postma DS, Kerstjens HA, Gosens R. Activation of WNT/β-catenin signaling in pulmonary fibroblasts by TGF-β_1 is increased in chronic obstructive pulmonary disease. *PLoS One* 2011;6:e25450.
14. Vasioukhin V, Fuchs E. Actin dynamics and cell-cell adhesion in epithelia. *Curr Opin Cell Biol* 2001;13:76–84.
15. Reya T, Clevers H. Wnt signalling in stem cells and cancer. *Nature* 2005;434:843–850.
16. Reynolds SD, Zemke AC, Giangreco A, Brockway BL, Teisanu RM, Drake JA, Mariani T, Di PY, Taketo MM, Stripp BR. Conditional stabilization of beta-catenin expands the pool of lung stem cells. *Stem Cells* 2008;26:1337–1346.
17. Drees F, Pokutta S, Yamada S, Nelson WJ, Weis WI. Alpha-catenin is a molecular switch that binds E-cadherin-beta-catenin and regulates actin-filament assembly. *Cell* 2005;123:903–915.
18. Zhang Y, Goss AM, Cohen ED, Kadzik R, Lepore JJ, Muthukumaraswamy K, Yang J, DeMayo FJ, Whitsett JA, Parmacek MS, *et al*. A Gata6-Wnt pathway required for epithelial stem cell development and airway regeneration. *Nat Genet* 2008;40:862–870.
19. Zhang L, Gallup M, Zlock L, Basbaum C, Finkbeiner WE, McNamara NA. Cigarette smoke disrupts the integrity of airway adherens junctions through the aberrant interaction of p120-catenin with the cytoplasmic tail of MUC1. *J Pathol* 2013;229:74–86.
20. Sun Z, Gong X, Zhu H, Wang C, Xu X, Cui D, Qian W, Han X. Inhibition of Wnt/β-catenin signaling promotes engraftment of mesenchymal stem cells to repair lung injury. *J Cell Physiol* 2014;229:213–224.
21. Kneidinger N, Yildirim AO, Callegari J, Takenaka S, Stein MM, Dumitrascu R, Bohla A, Bracke KR, Morty RE, Brusselle GG, *et al*. Activation of the WNT/β-catenin pathway attenuates experimental emphysema. *Am J Respir Crit Care Med* 2011;183:723–733.
22. Crosby LM, Waters CM. Epithelial repair mechanisms in the lung. *Am J Physiol Lung Cell Mol Physiol* 2010;298:L715–L731.
23. Jiang Z, Polverino F, Lao T, Qiu W, Gupta K, Mancini J, Cho M, Castaldi P, Guo F, Laucho-Contreras M, *et al*. The chronic obstructive pulmonary disease susceptibility gene Fam13a negatively regulates the β-catenin/Wnt pathway. Presented at Federation of American Societies for Experimental Biology Science Research Conferences for Lung Epithelium in Health & Disease. July 27-August 1, 2014, Saxtons River, VT.
24. Zhou X, Baron RM, Hardin M, Cho MH, Zielinski J, Hawrylkiewicz I, Sliwinski P, Hersh CP, Mancini JD, Lu K, *et al*. Identification of a chronic obstructive pulmonary disease genetic determinant that regulates HHIP. *Hum Mol Genet* 2012;21:1325–1335.
25. Testa G, Schaft J, van der Hoeven F, Glaser S, Anastassiadis K, Zhang Y, Hermann T, Stremmel W, Stewart AF. A reliable lacZ expression reporter cassette for multipurpose, knockout-first alleles. *Genesis* 2004;38:151–158.
26. Moghadaszadeh B, Rider BE, Lawlor MW, Childers MK, Grange RW, Gupta K, Boukedes SS, Owen CA, Beggs AH. Selenoprotein N deficiency in mice is associated with abnormal lung development. *FASEB J* 2013;27:1585–1599.
27. Laucho-Contreras ME, Taylor KL, Mahadeva R, Boukedes SS, Owen CA. Automated measurement of pulmonary emphysema and small airway remodeling in cigarette smoke-exposed mice. *J Vis Exp* 2015; 95:52236.
28. Wang Y, Zhou X, Zhu H, Liu S, Zhou C, Zhang G, Xue L, Lu N, Quan L, Bai J, *et al*. Overexpression of EB1 in human esophageal squamous cell carcinoma (ESCC) may promote cellular growth by activating beta-catenin/TCF pathway. *Oncogene* 2005;24: 6637–6645.
29. Rock J, Königshoff M. Endogenous lung regeneration: potential and limitations. *Am J Respir Crit Care Med* 2012;186:1213–1219.
30. Desai TJ, Brownfield DG, Krasnow MA. Alveolar progenitor and stem cells in lung development, renewal and cancer. *Nature* 2014;507: 190–194.
31. Lao T, Glass K, Qiu W, Polverino F, Gupta K, Morrow J, Mancini JD, Vuong L, Perrella MA, Hersh CP, *et al*. Haploinsufficiency of Hedgehog interacting protein causes increased emphysema induced by cigarette smoke through network rewiring. *Genome Med* 2015;7:12.

32. Guerassimov A, Hoshino Y, Takubo Y, Turcotte A, Yamamoto M, Ghezzo H, Triantafillopoulos A, Whittaker K, Hoidal JR, Cosio MG. The development of emphysema in cigarette smoke-exposed mice is strain dependent. *Am J Respir Crit Care Med* 2004;170:974–980.
33. Rahman I. Oxidative stress, chromatin remodeling and gene transcription in inflammation and chronic lung diseases. *J Biochem Mol Biol* 2003;36:95–109.
34. Chung KF. Cytokines as targets in chronic obstructive pulmonary disease. *Curr Drug Targets* 2006;7:675–681.
35. Chung KF, Adcock IM. Multifaceted mechanisms in COPD: inflammation, immunity, and tissue repair and destruction. *Eur Respir J* 2008;31:1334–1356.
36. Tamimi A, Serdarevic D, Hanania NA. The effects of cigarette smoke on airway inflammation in asthma and COPD: therapeutic implications. *Respir Med* 2012;106:319–328.
37. Owen CA. Proteinases and oxidants as targets in the treatment of chronic obstructive pulmonary disease. *Proc Am Thorac Soc* 2005;2: 373–385. [Discussion 394–375.]
38. Gill SE, Parks WC. Metalloproteinases and their inhibitors: regulators of wound healing. *Int J Biochem Cell Biol* 2008;40:1334–1347.
39. Owen CA. Roles for proteinases in the pathogenesis of chronic obstructive pulmonary disease. *Int J Chron Obstruct Pulmon Dis* 2008;3:253–268.
40. Atkinson JJ, Lutey BA, Suzuki Y, Toennies HM, Kelley DG, Kobayashi DK, Ijem WG, Deslee G, Moore CH, Jacobs ME, *et al*. The role of matrix metalloproteinase-9 in cigarette smoke-induced emphysema. *Am J Respir Crit Care Med* 2011;183:876–884.
41. Xu Y, Chen Y, Zhang P, Jeffrey PD, Shi Y. Structure of a protein phosphatase 2A holoenzyme: insights into B55-mediated Tau dephosphorylation. *Mol Cell* 2008;31:873–885.
42. Zou W, Zou Y, Zhao Z, Li B, Ran P. Nicotine-induced epithelial-mesenchymal transition via Wnt/β-catenin signaling in human airway epithelial cells. *Am J Physiol Lung Cell Mol Physiol* 2013;304: L199–L209.
43. Lee JM, Yang J, Newell P, Singh S, Parwani A, Friedman SL, Nejak-Bowen KN, Monga SP. β-Catenin signaling in hepatocellular cancer: implications in inflammation, fibrosis, and proliferation. *Cancer Lett* 2014;343:90–97.
44. Liu C, Kato Y, Zhang Z, Do VM, Yankner BA, He X. beta-Trcp couples beta-catenin phosphorylation-degradation and regulates Xenopus axis formation. *Proc Natl Acad Sci USA* 1999;96:6273–6278.
45. Zeng J, Liu D, Qiu Z, Huang Y, Chen B, Wang L, Xu H, Huang N, Liu L, Li W. GSK3β overexpression indicates poor prognosis and its inhibition reduces cell proliferation and survival of non-small cell lung cancer cells. *PLoS One* 2014;9:e91231.
46. Roose J, Huls G, van Beest M, Moerer P, van der Horn K, Goldschmeding R, Logtenberg T, Clevers H. Synergy between tumor suppressor APC and the beta-catenin-Tcf4 target Tcf1. *Science* 1999;285:1923–1926.
47. DasGupta R, Fuchs E. Multiple roles for activated LEF/TCF transcription complexes during hair follicle development and differentiation. *Development* 1999;126:4557–4568.
48. Beyer C, Reichert H, Akan H, Mallano T, Schramm A, Dees C, Palumbo-Zerr K, Lin NY, Distler A, Gelse K, *et al*. Blockade of canonical Wnt signalling ameliorates experimental dermal fibrosis. *Ann Rheum Dis* 2013;72:1255–1258.
49. Leow PC, Tian Q, Ong ZY, Yang Z, Ee PL. Antitumor activity of natural compounds, curcumin and PKF118-310, as Wnt/β-catenin antagonists against human osteosarcoma cells. *Invest New Drugs* 2010;28:766–782.
50. Lucey EC, Goldstein RH, Stone PJ, Snider GL. Remodeling of alveolar walls after elastase treatment of hamsters. Results of elastin and collagen mRNA in situ hybridization. *Am J Respir Crit Care Med* 1998;158:555–564.
51. Wright JL, Cosio M, Churg A. Animal models of chronic obstructive pulmonary disease. *Am J Physiol Lung Cell Mol Physiol* 2008;295: L1–L15.
52. Wright JL, Churg A. Animal models of cigarette smoke-induced chronic obstructive pulmonary disease. *Expert Rev Respir Med* 2010;4: 723–734.
53. Wang R, Ahmed J, Wang G, Hassan I, Strulovici-Barel Y, Hackett NR, Crystal RG. Down-regulation of the canonical Wnt β-catenin pathway in the airway epithelium of healthy smokers and smokers with COPD. *PLoS One* 2011;6:e14793.
54. Kim TH, Kim SH, Seo JY, Chung H, Kwak HJ, Lee SK, Yoon HJ, Shin DH, Park SS, Sohn JW. Blockade of the Wnt/β-catenin pathway attenuates bleomycin-induced pulmonary fibrosis. *Tohoku J Exp Med* 2011;223:45–54.
55. Li Y, Shi J, Yang J, Ma Y, Cheng L, Zeng J, Hao X, Ma C, Wang Y, Liu X. A Wnt/β-catenin negative feedback loop represses TLR-triggered inflammatory responses in alveolar epithelial cells. *Mol Immunol* 2014;59:128–135.
56. Tanjore H, Degryse AL, Crossno PF, Xu XC, McConaha ME, Jones BR, Polosukhin VV, Bryant AJ, Cheng DS, Newcomb DC, *et al*. β-catenin in the alveolar epithelium protects from lung fibrosis after intratracheal bleomycin. *Am J Respir Crit Care Med* 2013;187:630–639.
57. Aggarwal NR, Chau E, Garibaldi BT, Mock JR, Sussan T, Rao K, Rao K, Menon AG, D'Alessio FR, Damarla M, *et al*. Aquaporin 5 regulates cigarette smoke induced emphysema by modulating barrier and immune properties of the epithelium. *Tissue Barriers* 2013;1:e25248.
58. Lemjabbar H, Li D, Gallup M, Sidhu S, Drori E, Basbaum C. Tobacco smoke-induced lung cell proliferation mediated by tumor necrosis factor alpha-converting enzyme and amphiregulin. *J Biol Chem* 2003;278:26202–26207.
59. Muyal JP, Kotnala S, Bhardwaj H, Tyagi A. Effect of recombinant human keratinocyte growth factor in inducing Ras-Raf-Erk pathway-mediated cell proliferation in emphysematous mice lung. *Inhal Toxicol* 2014;26:761–771.
60. Fang X, Li K, Tao X, Chen C, Wang X, Wang L, Wang DC, Zhang Y, Bai C, Wang X. Effects of phosphoinositide 3-kinase on protease-induced acute and chronic lung inflammation, remodeling, and emphysema in rats. *Chest* 2013;143:1025–1035.
61. Arnold HK, Sears RC. A tumor suppressor role for PP2A-B56alpha through negative regulation of c-Myc and other key oncoproteins. *Cancer Metastasis Rev* 2008;27:147–158.
62. Li X, Yost HJ, Virshup DM, Seeling JM. Protein phosphatase 2A and its B56 regulatory subunit inhibit Wnt signaling in Xenopus. *EMBO J* 2001;20:4122–4131.
63. Seeling JM, Miller JR, Gil R, Moon RT, White R, Virshup DM. Regulation of beta-catenin signaling by the B56 subunit of protein phosphatase 2A. *Science* 1999;283:2089–2091.
64. Geraghty P, Hardigan AA, Wallace AM, Mirochnitchenko O, Thankachen J, Arellanos L, Thompson V, D'Armiento JM, Foronjy RF. The glutathione peroxidase 1-protein tyrosine phosphatase 1B-protein phosphatase 2A axis. A key determinant of airway inflammation and alveolar destruction. *Am J Respir Cell Mol Biol* 2013;49:721–730.
65. Jin Z, Chung JW, Mei W, Strack S, He C, Lau GW, Yang J. Regulation of nuclear-cytoplasmic shuttling and function of family with sequence similarity 13, member A (Fam13a), by B56-containing PP2As and Akt. *Mol Biol Cell* 2015;26:1160–1173.
66. Ding VW, Chen RH, McCormick F. Differential regulation of glycogen synthase kinase 3beta by insulin and Wnt signaling. *J Biol Chem* 2000;275:32475–32481.
67. Sutton LP, Rushlow WJ. The dopamine D2 receptor regulates Akt and GSK-3 via Dvl-3. *Int J Neuropsychopharmacol* 2012;15:965–979.
68. Li VS, Ng SS, Boersema PJ, Low TY, Karthaus WR, Gerlach JP, Mohammed S, Heck AJ, Maurice MM, Mahmoudi T, *et al*. Wnt signaling through inhibition of β-catenin degradation in an intact Axin1 complex. *Cell* 2012;149:1245–1256.
69. Morrisey EE, Cardoso WV, Lane RH, Rabinovitch M, Abman SH, Ai X, Albertine KH, Bland RD, Chapman HA, Checkley W, *et al*. Molecular determinants of lung development. *Ann Am Thorac Soc* 2013;10: S12–S16.
70. Lamontagne M, Couture C, Postma DS, Timens W, Sin DD, Paré PD, Hogg JC, Nickle D, Laviolette M, Bossé Y. Refining susceptibility loci of chronic obstructive pulmonary disease with lung eqtls. *PLoS One* 2013;8:e70220.
71. Fingerlin TE, Murphy E, Zhang W, Peljto AL, Brown KK, Steele MP, Loyd JE, Cosgrove GP, Lynch D, Groshong S, *et al*. Genome-wide association study identifies multiple susceptibility loci for pulmonary fibrosis. *Nat Genet* 2013;45:613–620.